



# Fate of ammonia emissions at the local to regional scale as simulated by the Community Multiscale Air Quality model

Robin L. Dennis<sup>1</sup>, Rohit Mathur<sup>1</sup>, Jonathan E. Pleim<sup>1</sup>, John T. Walker<sup>2</sup>

<sup>1</sup> National Exposure Research Laboratory, U.S. Environmental Protection Agency, Research Triangle Park, North Carolina, 27711 United States

<sup>2</sup> National Risk Management Research Laboratory, U.S. Environmental Protection Agency, Research Triangle Park, North Carolina, 27711 United States

## ABSTRACT

Atmospheric deposition of nitrogen contributes to eutrophication of estuarine waters and acidification of lakes and streams. Ammonia also contributes to fine particle formation in the atmosphere and associated health effects. Model projections suggest that  $\text{NH}_3$  deposition may become the major source of nitrogen deposition in the future. The regional transport of  $\text{NH}_3$  contributes to nitrogen deposition. Conventional wisdom for many is that a large fraction, or even all, of the  $\text{NH}_3$  emissions deposit locally, near their source as dry deposition, which we believe is incorrect. In this study we use a regional atmospheric model, the Community Multiscale Air Quality (CMAQ) model to identify the dominant processes that dictate the fate of  $\text{NH}_3$  and address the questions of how much  $\text{NH}_3$  deposits locally and what is the range of influence of  $\text{NH}_3$  emissions. The CMAQ simulation is for June 2002 with a 12-km grid size, covering the eastern half of the U.S. We study three different  $\text{NH}_3$  dry deposition formulations, including one that represents bi-directional  $\text{NH}_3$  air–surface exchange, to represent uncertainty in the  $\text{NH}_3$  dry deposition estimates. We find for 12-km cells with high  $\text{NH}_3$  emissions from confined animal operations that the local budget is dominated by turbulent transport away from the surface and that from 8–15% of a cell's  $\text{NH}_3$  emissions dry deposit locally back within the same cell. The CMAQ estimates are consistent with local, semi-empirical budget studies of  $\text{NH}_3$  emissions. The range of influence of a single cell's emissions varies from 180 to 380 kilometers, depending on the dry deposition formulation. At the regional scale, wet deposition is the major loss pathway for  $\text{NH}_3$ ; nonetheless, about a quarter of the  $\text{NH}_3$  emissions are estimated to transport off the North American continent, an estimate that is not sensitive to the uncertainty in dry deposition.

## Keywords:

Ammonia deposition  
Ammonia emission influence range  
Atmospheric budget  
Modeling  
CMAQ

## Article History:

Received: 24 March 2010

Revised: 02 July 2010

Accepted: 06 July 2010

## Corresponding Author:

Robin L. Dennis

Tel: +1-919-541-2870

Fax: +1-919-541-1379

E-mail: dennis.robin@epa.gov

© Author(s) 2010. This work is distributed under the Creative Commons Attribution 3.0 License.

doi: 10.5094/APR.2010.027

## 1. Introduction

Atmospheric deposition of reactive nitrogen is a source of nutrient enrichment and one of the sources of acidification that, as stressors, cause deleterious impacts on terrestrial and aquatic ecosystems (Driscoll et al., 2001; Dennis et al., 2007; Lovett and Tear, 2008). Oxidized nitrogen from emissions of nitrogen oxides ( $\text{NO}_x$ ) and reduced nitrogen from emissions of ammonia ( $\text{NH}_3$ ) are the main contributors to the reactive nitrogen deposition budget. Reactive nitrogen emissions have increased significantly over the last century (Vitousek et al., 1997; Galloway and Cowling, 2002) leading to increases in both oxidized nitrogen ( $\text{NO}_y$ ) and  $\text{NH}_x$  ( $= \text{NH}_3 + \text{NH}_4^+$ ) deposition. Ammonia is also an important ingredient in inorganic fine particle mass formation and the resulting human health impacts (Seinfeld and Pandis, 1998). The importance of  $\text{NH}_3$  as a stressor is expected to increase as emissions of  $\text{NO}_x$  are projected to decrease due to Clean Air Act regulations while emissions of  $\text{NH}_3$  are expected to continue to increase (Pinder et al., 2008).

It is important in ecosystem studies involving the nitrogen budget to properly account for all nitrogen emissions and deposition. In contrast to oxidized nitrogen, the transport of  $\text{NH}_3$  is often not recognized even though reduced nitrogen source–receptor matrices are routinely calculated for Europe (Tarrason and Nyiri, 2008) and historical  $\text{NH}_3$  modeling experience exists in Europe (van Pul et al., 2009). The conventional wisdom among a variety of researchers is that local  $\text{NH}_3$  emissions are largely, or even fully, deposited back onto the source area (Asman, 1998;

Castro et al., 2001; Howarth et al., 2002; Dumont et al., 2005; Clarisse et al., 2009). We believe that this conventional wisdom is incorrect. The range of influence of  $\text{NH}_3$  emissions has an important bearing on identification of the source regions impacting receptors. Airsheds for coastal estuaries have been estimated for oxidized and reduced nitrogen using earlier models and for  $\text{NH}_3$  the estimated airsheds were multistate in size (Paerl et al., 2002). Given the continued prevalence of the conventional wisdom regarding the transport scales of  $\text{NH}_3$  emissions, a more detailed investigation of the dominant processes governing the fate of  $\text{NH}_3$  at the regional scale is needed.

The fate of  $\text{NH}_3$  through wet and dry deposition is expected to have an important effect on the range of influence of  $\text{NH}_3$  emissions. Model estimates of ammonia dry deposition are highly uncertain for North American conditions, in part, because most empirical studies have been conducted in Europe where significant effort has been devoted to quantify and parameterize the dry deposition velocity of  $\text{NH}_3$  for a variety of surface conditions (Duyzer et al., 1992; Sutton et al., 1993; Wyers and Erisman, 1998; Milford et al., 2001). Sutton et al. (1994) summarize several observational studies and report typical  $V_d$  values in the range of  $0.5\text{--}5\text{ cm s}^{-1}$  for a variety of natural and forested ecosystems. The uncertainty is compounded by the recognition that  $\text{NH}_3$  air–surface exchange is bi-directional (Flechard et al., 1999; Nemitz et al., 2001; Walker et al., 2008). It is useful to gain insight into the 3D  $\text{NH}_3$  atmospheric budget given the uncertainty in  $\text{NH}_3$  deposition parameterizations for North American conditions (Mathur and Dennis, 2003; Phillips et al., 2004; Walker et al., 2006; Aneja et al.,

2008). In this paper we examine the 3D fate of  $\text{NH}_3$  emissions in light of the uncertainty in  $\text{NH}_3$  air–surface exchange, including bi-directional air–surface exchange. Air quality model output of pollutant concentrations and deposition typically only reflects the cumulative effect of all physical and chemical processes that influence the  $\text{NH}_3$  budget. We examine the fate of  $\text{NH}_3$  emissions with the help of an “instrumented”, regional-scale numerical air quality model in which additional process-level information related to fate and the mass budget is output (such as advection, vertical diffusion, emissions, and deposition) (see the Supporting Material (SM), for a more complete description).

The objective is to address the following questions: (1a) what fraction of the local  $\text{NH}_3$  emissions deposit within the cell into which they are emitted; (1b) what is the fate of the local  $\text{NH}_3$  emissions at the surface and in the total column over the emitting cell; (2) how far downwind do  $\text{NH}_3$  emissions from a high emission cell have a significant impact (range of influence); and (3) what is the fate of regional  $\text{NH}_3$  emissions from all sources; what fraction of the emissions is transported out of the domain.

First, we briefly describe the Community Multiscale Air Quality model (CMAQ) and its ability to represent relevant deposition and air concentration gradients, with details provided in the SM. We next develop a set of sensitivity cases to address dry deposition uncertainty and describe the study approach. We then present results relative to the three questions posed above and conclude with a discussion of the results.

## 2. Model Description

### 2.1. Summary of CMAQ description and evaluation

CMAQ is a 3-dimensional grid model that simulates the transport, transformation and wet and dry deposition of a full suite of species. Details of the simulated physical and chemical processes are provided in Byun and Schere (2006) and the references therein. Further detail on the dry deposition algorithms is given in Section 3.1. The “instrumentation” of CMAQ is described in the Supporting Material and details are available in Gipson (1999). The meteorological inputs for this study are derived from the Fifth Generation Penn State/NCAR Mesoscale Model (MM5) (Grell et al., 1994). The CMAQ horizontal grid size was 12 x 12 kilometers with

vertical extent to 16 kilometers; the domain for the study is shown in Figure 1; the simulation period is June 2002.

Comparisons of CMAQ outputs with annual National Atmospheric Deposition Program (NADP) data and Chemical Speciation Network (CSN) and Clean Air Status and Trends Network (CASTNET) data show CMAQ is able to capture the main spatial pattern and magnitude of  $\text{NH}_3$  wet deposition and pattern of ambient concentrations across the continental U.S. Regional gradients of  $\text{NH}_3$  concentrations across North Carolina between a location with high animal operation emissions and a location in a low emission area are captured reasonably well by CMAQ (for July 2004: Observed:  $14.0$  vs.  $1.2 \mu\text{g m}^{-3}$ ; CMAQ:  $13.7$  vs.  $1.1 \mu\text{g m}^{-3}$ ) (see the SM for more detail).

### 2.2. Dry deposition uncertainty

The net  $\text{NH}_3$  dry net flux has an important influence on the balance between emissions, sinks, and transport. Deposition velocity data are sparse, especially in the U.S., against which to compare the CMAQ estimates. As noted above, Sutton et al. (1994) reported typical  $V_d$  values for  $\text{NH}_3$  in the range of  $0.5$ – $5 \text{ cm s}^{-1}$  for a variety of natural and forested ecosystems. Asman (2001) estimated an average  $V_d$  of  $1.2 \text{ cm s}^{-1}$  for low vegetation landscapes and suggested that for forests the  $V_d$  could be of the order of  $2.5 \text{ cm s}^{-1}$ . Many European studies (e.g. Flechard et al., 1999; Nemitz et al., 2001), acknowledge the existence of bi-directional air–surface exchange. For the U.S., Rattray and Sievering (2001) reported daytime  $V_d$ 's of  $1.7$ – $2.3 \text{ cm s}^{-1}$  over alpine tundra and Phillips et al. (2004) reported summertime nighttime values of  $V_d$  of  $0.76 \pm 1.7 \text{ cm s}^{-1}$  and daytime values of  $3.9 \pm 2.8 \text{ cm s}^{-1}$  for unfertilized grass close to animal operations, with an average  $V_d$  of  $1.9 \text{ cm s}^{-1}$ . The uncertainty in the Phillips et al. (2004) estimates is high and only for about 60% of the measurements was there an unambiguous flux to the surface. Walker et al. (2006) report a mean  $V_d$  of  $0.13 \text{ cm s}^{-1}$  over fertilized soybeans, the low net flux stemming from the bi-directional exchange of  $\text{NH}_3$  and large cuticular resistance due to  $\text{NH}_3$  accumulation. Pryor et al. (2001) reported  $\text{NH}_3$  emissions instead of deposition on 3 of 17 days above a forest in the Midwestern U.S. Recent flux measurements over fertilized corn in North Carolina show significant periods of  $\text{NH}_3$  emissions during a diurnal cycle. Thus, bi-directional exchange of  $\text{NH}_3$  needs to be considered.

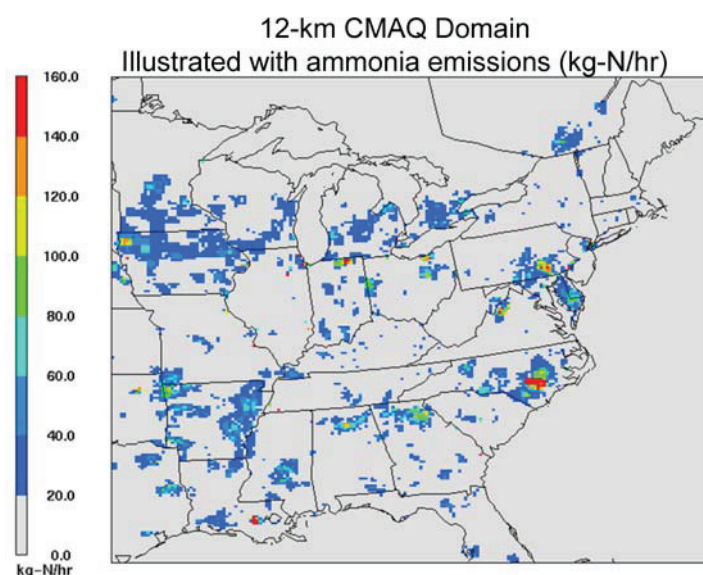


**Figure 1.** Map of the 12 km x 12 km June 2002 hourly average  $\text{NH}_3$  emissions ( $\text{kg-N hr}^{-1}$ ) showing the areas with high emissions and the CMAQ domain of the study.

Figure 2 presents the median of the  $V_d$ 's computed by CMAQ together with the 95<sup>th</sup> and 5<sup>th</sup> percentile values from cells across the modeling domain by hour for  $\text{HNO}_3$ ,  $\text{NH}_3$  and  $\text{SO}_2$  for a randomly selected day in June 2002. The figure shows that the median  $V_d$  for  $\text{NH}_3$  being computed by CMAQ is between that of  $\text{HNO}_3$  and  $\text{SO}_2$ , but closer to  $\text{HNO}_3$ . The CMAQ diurnal median  $\text{NH}_3$   $V_d$  range across the domain seems consistent with sparse observations, spanning from  $0.25 \text{ cm s}^{-1}$  to  $2.5 \text{ cm s}^{-1}$ . The 95<sup>th</sup> percentile values in Figure 2 for  $\text{HNO}_3$  and  $\text{NH}_3$  are very comparable and exceed  $5 \text{ cm s}^{-1}$ . Rattray and Sievering (2001) report comparable  $\text{HNO}_3$  and  $\text{NH}_3$   $V_d$ 's for tundra, but at levels of approximately  $2 \text{ cm s}^{-1}$ . However, given the bi-directional nature of  $\text{NH}_3$  flux at the surface, a unidirectional form is likely to yield deposition that is biased high, affecting the  $\text{NH}_3$  budget and the range of influence of  $\text{NH}_3$  emissions. Hence, the current flux parameterization for  $\text{NH}_3$  is expected to provide an upper bound for an assessment of the  $\text{NH}_3$  budget, but it would be useful to have a bi-directional  $\text{NH}_3$  flux formulation and to have a “lower bound” uni-directional flux estimate for comparison to help address the uncertainty.

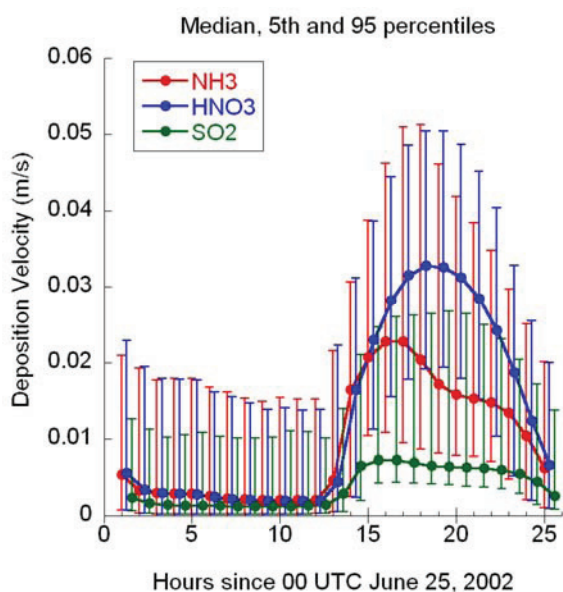


**Figure 2.** Diurnal profile of median and 5<sup>th</sup> & 95<sup>th</sup> percentiles of  $V_d$ 's calculated by CMAQ across the model domain for June 25, 2002 in Greenwich Mean Time, for  $\text{NH}_3$ ,  $\text{HNO}_3$  and  $\text{SO}_2$ . To see the bars  $\text{HNO}_3$  is on the hour,  $\text{NH}_3$  is offset ahead and  $\text{SO}_2$  offset behind each hour.

### 3. Design of the Modeling Experiment

This study is designed to conduct CMAQ simulations for June 2002 with process analysis for assessing the major components of the  $\text{NH}_3$  fate/budget, for three different cases of dry  $\text{NH}_3$  flux, two of which represent an upper and a lower estimate of the flux using uni-directional algorithms. The third case is a prototype representation of bi-directional  $\text{NH}_3$  flux in CMAQ. The range of cases is intended to provide a sense of the  $\text{NH}_3$  budget and its sensitivity to the uncertainties in removal via dry deposition. This design, which assumes the current formulation for  $\text{NH}_3$  flux represents the upper bound, requires implementation of a prototype bi-directional  $\text{NH}_3$  flux algorithm for CMAQ to more completely represent the flux processes. It then requires selection of an appropriate uni-directional flux formulation, based on another species, to be applied to  $\text{NH}_3$  to provide a lower estimate, and potentially, on average, a lower bound for natural systems.

#### 3.1. Current $\text{NH}_3$ flux algorithm

The uni-directional  $\text{NH}_3$  flux model is the dry deposition model (M3dry) in the CMAQ model system (Pleim et al., 2001). This

model uses the resistance analogy as the basic approach to formulation, as shown in Figure S1 (see the SM). The aerodynamic and surface layer resistances are governed, respectively, by turbulent transfer from the atmosphere to the receptor and molecular diffusion across the laminar sub-layer of air at the receptor surface (plant or ground). Fluxes to the foliage are controlled by the cuticular resistance and the stomatal resistance in series with the mesophyll resistance. The M3dry model uses bulk stomatal and aerodynamic resistances from the Pleim–Xiu–land–surface model (Pleim and Xiu, 1995; Xiu and Pleim, 2001) used in MM5. The surface resistance (cuticle and ground) is scaled by reactivity for dry surfaces and effective Henry's law constants for wet surfaces. The CMAQ results from the base, M3dry model formulation are termed Base for this study.

#### 3.2. Bi-directional $\text{NH}_3$ flux algorithm

To create the bi-directional capability, the dry deposition sink is replaced by a compensation point model in vertical diffusion in the CMAQ model. This two-layer canopy compensation point model formulation follows Nemitz et al. (2001). With the flux model in CMAQ, air concentrations can be compared to compensation points. The compensation point for  $\text{NH}_3$  is the gas phase concentration at equilibrium with liquid  $\text{NH}_3$  concentration in the stomatal cavities ( $\chi_s$ ) and with  $\text{NH}_3$  concentrations in the soil ( $\chi_g$ ). For plants, the stomatal compensation point is a function of temperature and the ratio of  $\text{NH}_4^+$  to  $\text{H}^+$  in the stomatal cavity. The latter ratio is termed the leaf or soil emission potential,  $\Gamma$ , which controls canopy-scale  $\text{NH}_3$  fluxes. The resistance analog model was modified to include compensation concentrations in the stomatal cavities and soil, as shown in Figure S1 (see the SM). The leaf emission potential is  $\Gamma_s$  and the soil emission potential is  $\Gamma_g$ . The compensation point model is semi-empirical and relies heavily on field measurements for both development and testing. Development of the prototype is based on summer 2002 field data from Duplin County fertilized soybeans (Walker et al., 2006). Gamma values,  $\Gamma$ , are specified by broad land-use (LU) category. A  $\Gamma_s = 1000$  is assumed for fertilized crops; for non-fertilized crops and natural (or non-agricultural) vegetation  $\Gamma_s = 100$ ; and for ground  $\Gamma_g = 0.8 \Gamma_s$ . These are very general recommendations that come from the Edinburgh research group (Loubet et al., 2009) and adapted by Walker et al. (2006) and Walker et al. (2008). The Edinburgh group did not distinguish different crops. Research based on North Carolina bi-directional flux studies, currently in process, will better distinguish differences in the magnitude of  $\Gamma$  for different crops for incorporation into CMAQ for public release. Aggregate  $\Gamma$  values for each grid cell are weighted according to fractional LU coverage. The CMAQ results from the bi-directional formulation are identified as Bi-Di.

#### 3.3. Lower estimate $\text{NH}_3$ flux algorithm

The purpose of the lower estimate is to provide a range to better depict the sensitivity of the analysis of the fate of  $\text{NH}_3$  to the uncertainty in dry deposition. We selected  $\text{SO}_2$  to represent the lower bound  $V_d$  because  $\text{SO}_2$  has similar surface interactions as  $\text{NH}_3$ , but its  $V_d$  is smaller. The M3dry model structure for  $\text{SO}_2$  deposition is the same as for  $\text{NH}_3$  and both are responsive to surface wetness.  $\text{SO}_2$  is less sticky than  $\text{NH}_3$  and somewhat less water soluble resulting in  $V_d$ 's that are smaller than but similar to those of  $\text{NH}_3$  (see Figure 2). This is confirmed by Figure S5, a map of the maximum  $V_d$  across the domain for the randomly selected day of Figure 2, that is shown in the SM. Thus, the  $V_d$ 's for  $\text{SO}_2$  were applied to  $\text{NH}_3$  concentrations for the “lower bound” estimates. The CMAQ results from this formulation are identified as  $\text{SO}_2 V_d$ .

#### 3.4. Budget analysis approach

Results were developed and analyzed for June 2002 to address the three study questions. June was chosen because  $\text{NH}_3$  emissions

are high (enhanced relative to the annual average) and crops are fully leafed out. The analysis focuses on cells with much higher than average  $\text{NH}_3$  emissions, because of the potential for significant impacts. From the U.S. EPA National Emissions Inventory for 2002, emissions from fertilized crops account for 35% and 28% of the annual and summer  $\text{NH}_3$  emissions, respectively; the great majority come from animal operations. Grid cells with more than 90% of the emissions from animal operations had much higher emission rates and were more numerous than cells with more than 90% from fertilizer application. Thus, we focused on  $\text{NH}_3$  rich cells associated with animal operations for this study. Exploration of base results for 12 rural high-emission cells and 8 urban cells indicated that the agriculturally-related high emission cells tended to have a higher fraction of their  $\text{NH}_3$  emissions dry deposited in the emitting cell than urban cells (15–25% versus 10–15%, respectively). The difference is mainly due to the influence of emissions from neighboring cells. Deposition velocities were not substantially different across the cells, including non-agriculture–non-urban cells, because urban areas in the model are assumed to have vegetation, to have surface roughness comparable to deciduous forests, and to develop wet surfaces comparable to other land use types.

The amount of deposition in a cell has two components: deposition from local, within-cell emissions and deposition from emissions outside the cell. We want to eliminate the second influence for this analysis. With process analysis alone we only obtain a calculation of the net rate of deposition or transport in a cell and cannot distinguish the portions of the budget solely associated with the emissions from the single cell of interest. To remove the influence of the neighboring cells, we increased the  $\text{NH}_3$  emissions in the cell of interest, re-simulated the monthly budgets and then subtracted the base case results from the enhanced  $\text{NH}_3$  emissions case to obtain the true net budget for the single cell. Increasing emissions in  $\text{NH}_3$  rich cells should not affect the relative budget estimates for the single cell because the relative process rates are not changed by a change in emissions. We tested several  $\text{NH}_3$  emissions increases between 2 and 7 times higher than the base and confirmed the fraction dry depositing, in the single cell is invariant with respect to the emission rate in the single cell, providing a robust examination of the relative importance of the individual processes. Finding no relation also indicates that sulfate availability does not matter much in these high emission cells associated with animal operations because there is so much  $\text{NH}_3$  available (extremely  $\text{NH}_3$  rich). In fact, if the deposition rates are nominally independent of grid resolution over small relatively homogeneous domains, then the fraction of emissions dry depositing for a single cell analysis also is nominally independent of model grid resolution (using smaller grid sizes).

When cells were isolated from the emissions in neighboring cells the fraction of cell emissions dry depositing for Sampson County, NC and Lancaster County, PA was 15.4% and 16.3%, respectively. The Lancaster County cell was chosen as another cell with similarly localized emissions due to confined animal operations to check that the isolated deposition fraction of Sampson County could be approximately reproduced elsewhere. The June budget analyses for the first two study questions were calculated for the emissions from a single, isolated cell through the brute-force sensitivity-difference calculation. We chose a cell in Sampson County, NC to study because it has high  $\text{NH}_3$  emissions, due to agricultural confined animal operations. This cluster of cells in NC has high emissions relative to other cells within several hundred kilometers. Figure 1 illustrates the monthly  $\text{NH}_3$  emission rates for June 2002 for the modeling domain and shows the high emissions region in NC.

## 4. Results

Simulations with CMAQ configured in three versions, Base,  $\text{SO}_2\text{V}_d$  and Bi-Di, were performed with process analysis to attribute

the net result to each process. This provides quantitative information on net concentration gains and losses in a cell and by which process it occurred. The process analysis results were combined into monthly averages and deposition results were summed to provide monthly deposition values. The process budgets were computed for surface cells, for the vertical column above each cell or averaged over a regional domain of vertical columns. The study questions are addressed in turn in the next section.

### 4.1. Local fate of local $\text{NH}_3$ emissions

**Fate of local  $\text{NH}_3$  emissions at the surface.** To calculate the budget of the local  $\text{NH}_3$  emissions at the surface, we use the process analysis results for  $\text{NH}_3$  for the Sampson County surface cell after the base case was subtracted from the single cell enhanced  $\text{NH}_3$  emissions case. The gains in  $\text{NH}_3$  are due to  $\text{NH}_3$  emissions (into cell bottom) and the  $\text{NH}_3$  losses are due to dry deposition (out cell bottom), net horizontal advection (out cell sides), vertical advection and diffusion (out cell top), and chemical conversion of  $\text{NH}_3$  to particulate  $\text{NH}_4^+$ . The budget results are shown in Figure 3. The dry deposition is only a fraction of the total emissions into the cell: 7.7% and 15.4% for the  $\text{SO}_2\text{V}_d$  and the base cases, respectively. The dry deposition fraction is sensitive to the rate of the deposition, the fraction for the  $\text{SO}_2\text{V}_d$  case is half that of the base case. The fraction dry depositing in the Bi-Di case is 8.4%, close to the  $\text{SO}_2\text{V}_d$  case. Because the chemical conversion is so small these results also hold for  $\text{NH}_x = \text{NH}_3 + \text{NH}_4^+$ .

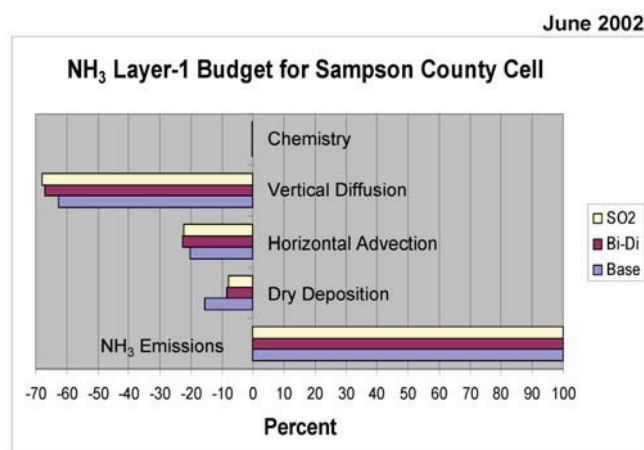


**Figure 3.** Bar chart of the  $\text{NH}_3$  layer-1 budget for the single, isolated Sampson County cell for June 2002:  $\text{SO}_2 - \text{SO}_2\text{V}_d$ ; Bi-Di = Bi-directional; Base = M3dry. Layer 1 nominally 38 m.

The fate of  $\text{NH}_3$  (and  $\text{NH}_x$ ) at the surface is dominated by turbulent diffusion (vertical mixing). Turbulent mixing transports a majority of the surface  $\text{NH}_3$  emissions up and away from the surface and into the atmospheric mixed layer. As shown in Figure 3, about 2/3rds of the emissions are moved aloft for all three cases. The magnitude of the horizontal transport, more than 20% for all three cases, indicates that cells with high emissions can influence the magnitude of the concentrations of adjacent or neighboring cells.

The three estimates from the CMAQ simulations for a summer month are that the local dry deposition flux ranges from 7.7–15.4% of the local emissions, with the bi-directional estimate at the lower end of the range. A few empirically-based estimates of the fraction of local  $\text{NH}_3$  emissions dry depositing locally from single high emission areas (confined animal operations) are available to compare to the spread of CMAQ estimates made in this study. Reported studies are for annual emissions. Fowler et al. (1998) estimated the fraction of annual  $\text{NH}_3$  emissions depositing within 300 m of a poultry facility surrounded by a forest in Scotland to be 3–10% and inferred the fraction out to 1.2 km to be around 10%.

Walker et al. (2008), using a two-layer bi-directional dry deposition model estimated that 7.8–13.3%, with a best estimate of 10.4%, of annual hog farm emissions dry deposited over the nearest 500 m. Further model analysis of the Walker et al. (2008) data for summer-time conditions indicated the fraction dry depositing is expected to peak at 13.5% at about 2.5 km from the farm because fertilized crops start influencing the bi-directional results at longer distances. European model studies have a wide range of estimates, suggesting that from 2% to 60% of the emissions deposit within short distances (Loubet et al., 2009). The CMAQ fractions are quite consistent with the empirically-based results, even though for a summer period. We do expect the fractions might be lower in winter. Since the average meteorology is similar across a grid cell, then we expect the process rates will not vary substantially across the grid cell if the land cover heterogeneity is not large (see the SM). Then, the fraction of emissions depositing, mixing and transporting will be moderately independent of grid size, similar to what was found in the above Walker et al. (2008) calculations. Thus, we expect CMAQ estimates of the fraction that dry deposits will be similar at finer grid resolutions consistent with the domains of these studies and the empirically-based estimates are considered to provide some ground truth against which to judge the CMAQ results.

#### Fate of high emitting cell emissions in total column above the cell.

Calculation of the total column budget above a cell allows us to construct information on what is happening above the surface. Importantly, the column resultant allows us to unambiguously estimate wet deposition as a loss process and include it in the analysis. We compute the fraction of the emissions introduced that are “lost” due to chemistry, long-range horizontal transport, and wet deposition in addition to dry deposition. The dry deposition has the same fraction as for the analysis at the surface. Budget results are shown in Figure S6 (see the SM). Once aloft, most of the  $\text{NH}_3$ , between 82–89%, is transported by horizontal advection away from the high emitting cell and a small fraction, 2.1–2.2%, is converted to aerosol  $\text{NH}_4^+$  before it is advected away. For this particular time period and location, only a small fraction (0.57–0.58%) of the emitted  $\text{NH}_3$  in this cell is wet deposited back to the surface. Mainly, once aloft, the  $\text{NH}_3$  from this high emitting cell undergoes horizontal transport, which is indicative of involvement in long-range transport.

#### 4.2. Range of influence of $\text{NH}_3$ emissions from a high emitting cell

Since we have found that most of the local surface emissions are not deposited locally but are involved in long range transport, then the question follows: over what spatial extent are the emissions expected to have an important impact? To address this question, an operational definition for the range of influence needs to be developed because the concentrations/deposition from a source decline with distance and become very diffuse to the point that the impact from that source is insignificant. A cutoff point must be established to create the operational definition. We defined the cutoff point for the range of influence to be the distance by which 50% of the emissions from the source have deposited. This is different than, but very consistent with the earlier definition of Dennis (1997) who first summed up the domain-wide deposition from a source and then defined the range of influence as the distance from the maximum deposition cell by which two-thirds of that source's domain-wide total deposition is deposited. The consistency between the two operational definitions will become apparent in the next section. The current definition is much easier to implement.

We subtracted the base case from the enhanced  $\text{NH}_3$  emissions case, as noted in Section 4.1 to isolate the analysis to the influence from a single cell, and accumulated the wet and dry deposition as a function of increasing distance from the isolated cell. Rather than taking average transport by compass direction into account to develop the accumulation, we simply incremented

a cell at a time in the four directions from the central cell in an expanding square and accumulated the deposition for each square. The results of the range of influence calculations are shown in Figure 4 for the three dry deposition algorithm cases. The distance on the x-axis is the perpendicular distance from the center cell to a side of the box. At 500 km on the graph each side of the box is 1 000 km.

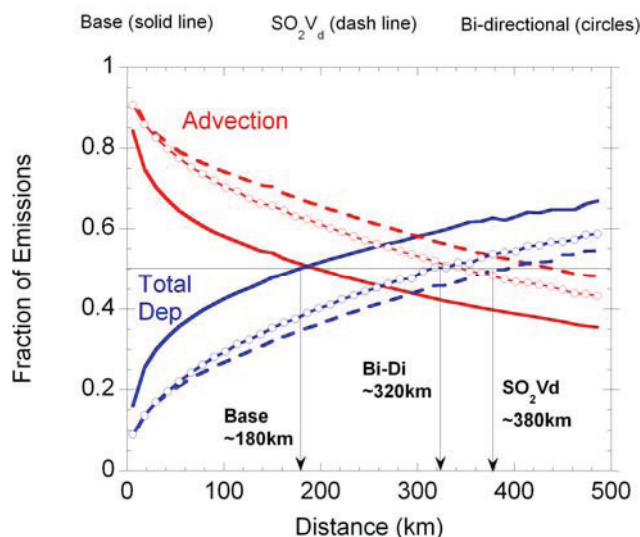


**Figure 4.** Range of influence of  $\text{NH}_3$  emissions from the single, isolated Sampson County, NC cell.

The model process analysis indicates that there is long-range transport of  $\text{NH}_3$  emissions. The range of influence depends significantly on the magnitude of the wet plus dry deposition flux. The range of influence is the shortest for the base case, approximately 180 km and the farthest for the  $\text{SO}_2\text{V}_d$  case, approximately 380 km. The range of the Bi-Di case is between the other two, approximately 320 km, but much closer to the  $\text{SO}_2\text{V}_d$  case. The range of the  $\text{SO}_2\text{V}_d$  case is approximately twice that of the base case. The 180 km range covers almost all of eastern North Carolina, and the 380 km range covers most of Virginia, North Carolina and South Carolina, reaching to Washington D.C. and covering a majority of the Chesapeake Bay. The results are particular to June 2002 and the meteorology in the southeast of the country.

#### 4.3. Regional fate of regional $\text{NH}_3$ emissions from all sources

All of the emissions sources and loss processes are acting together over a regional domain to produce a net result: the in situ environment that we observe. Emissions are continually being added to an air mass column as it is transported and the concentrations are continually being affected by inputs and losses. The model with process analysis can help us to understand what we ultimately expect to happen from a regional perspective. We found it instructive to start with the local budget and build up to the regional budget. We do this by computing and tracking the monthly average process analysis outputs and resulting budget in horizontally-expanding 3D volumes. Starting with the single column over the high emission cell and adding a new set of columns around the perimeter (4 sides) and averaging anew the properties for each new volume we can illuminate the transition from local to regional budgets. The budget is assessed for the vertical extent of the model to follow wet deposition and transport as well as dry deposition. As the size of the 3D box increases, the average air mass history time increases. This gives time for chemical conversion of  $\text{NH}_3$  to  $\text{NH}_4^+$  to take place as well as wet deposition and cleansing of the air mass contents. To follow the ultimate fate of the  $\text{NH}_3$  emissions at the broad regional scale, the budget for this analysis is tracked as  $\text{NH}_x$ .

The result of the expanding box budget analysis centered at the high emission cell in NC, but now including the  $\text{NH}_3$  emissions from all cells in each box, is shown in Figure 5. Dry deposition dominates the local loss process, but it soon plateaus and for the bi-directional implementation the dry deposition fraction peaks and then goes to a lower level before it plateaus. Soon (100–150 km out from the center) wet deposition catches up and then surpasses dry deposition to become the dominant regional loss process. By the regional air mass history time most of the  $\text{NH}_x$  budget is in the form of  $\text{NH}_4^+$ , explaining the dominance of wet deposition over dry deposition.

Expanding out 500 km from the center of analysis achieves an integration of the budget processes that has become regionally representative. The fractions at 500 km are very close to those computed for the entire modeling domain. Eventually the transport out of the expanding, regional box merges for all three cases and appears to stabilize at about 25%, suggesting that about a quarter of the regional emissions are expected to leave the domain. The transport out of the domain is relatively insensitive to the uncertainty in  $\text{NH}_3$  deposition. Wet and dry deposition differences for the 3 sensitivity cases offset each other nearly equally in the budget.

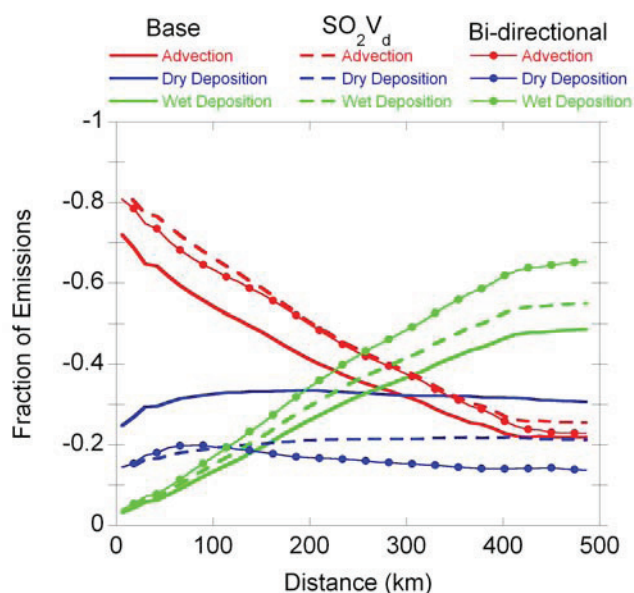


**Figure 5.** Cumulative regional  $\text{NH}_3$  budget of advection, wet- and dry-deposition, calculated for an expanding box starting at the high-emitting Sampson County, NC cell.

## 5. Discussion

The surface budgets developed and presented here are typical of most other  $\text{NH}_3$  emissions source regions associated with agricultural animal operations. While the fraction of  $\text{NH}_3$  emissions locally deposited is sensitive to the uncertainty in  $\text{NH}_3$  dry deposition, the message is still that vertical turbulent diffusion away from the surface is dominant and only a small fraction deposits locally. For a variety of locations across the domain, for which  $\text{NH}_3$  emission rates varied by a factor of 10, the fraction of  $\text{NH}_3$  emissions depositing in the same cell ranged from 5% to 20%. This analysis suggests a nominal value for the fraction of  $\text{NH}_3$  emissions dry depositing of 10% with a plausible range of 5% to 20%. Urban areas had smaller nominal dry deposition fractions for non-isolated cells than the agriculturally-related high emissions areas (10–15% versus 15–25% for the base case), but the emissions in neighboring cells of urban areas are also smaller leading to less distortion of the non-isolated deposition fraction estimate. Sampson County's net horizontal transport fraction increased from 7% to 20% when the cell was isolated (via subtraction of the base

case from the enhanced  $\text{NH}_3$  emissions case) and the nominal fraction dry depositing decreased from 24.5% to the uninflated estimate of 15.4%. Thus, an estimate of 10% for urban areas appears reasonable as well.

The range of influence of a single cell's emissions is sensitive to the uncertainty in  $\text{NH}_3$  dry deposition, varying by a factor of two. These uncertainties need to be reduced to provide a better estimate of the range of influence of the  $\text{NH}_3$  emissions. The estimates of the range of influence are for periods when plants are leafed out and fertilizer is assumed to be applied. They are expected to be somewhat different for winter and fallow periods. The magnitude of the difference will depend on the ground and foliage flux characteristics, including the relative importance of cuticular and stomatal resistances and the seasonality of ground and foliage emission potentials ( $I$ ), which govern the magnitude and temperature dependence of fluxes. Potentially the sensitivity to uncertainty will not be as large in these other time periods. There could be some influence of different partitioning of  $\text{NH}_x$  at different locations, but because wet and dry deposition counter balance each other we do not see much evidence of such an effect here. In spite of the uncertainties, the model analysis indicates that the range of influence of  $\text{NH}_3$  emissions can span hundreds of kilometers, and is not just a local-scale phenomenon.

For this study, the fraction of domain-wide  $\text{NH}_3$  emissions that is transported off the continent is relatively insensitive to the uncertainty in  $\text{NH}_3$  dry deposition, varying between 23 and 28%. Changes in dry deposition within the domain are compensated by a wet deposition change. Thus, this result appears to be fairly robust even with the deposition uncertainties. This estimate may be influenced by the boundary conditions aloft, but we believe this influence will be small.

A sensitivity study to explore the source of differences between the  $\text{NH}_3$  bi-directional and uni-direction flux formulations indicates clearly that the essential bi-directional elements driven by the compensation points are making the real difference between the two formulations. The differences in fluxes are not caused by differences in resistance parameter values. There is currently a large uncertainty in the bi-directional formulation associated with the estimation of  $\Gamma$ , the emissions potential due to the existence of compensation points. Nonetheless, we can learn much about the  $\text{NH}_3$  budget in spite of these uncertainties.

High priority research is ongoing to improve the bi-directional parameterization and the estimates of the leaf and soil gammas across different cropping regions and throughout the year. We are developing a software tool to estimate the soil  $\Gamma$  associated with fertilizer application. When we have a spatially and temporally varying  $\Gamma_g$ , we will investigate the emissions budgets for fertilized fields, as well as reexamine the animal operation emission budgets, as this will be of interest. Work to examine the seasonality of single cell budgets and their range of influence is continuing.

## Acknowledgements

The 2004  $\text{NH}_3$  data was from a study led by Wayne Robarge of NC State University. This paper has been reviewed in accordance with the U.S. Environmental Protection Agency's peer and administrative review policies and has been approved for publication. Approval does not signify that the contents necessarily reflect the views and policies of the Agency, nor does the mention of trade names or commercial products constitute endorsement or recommendation for use.

## Supporting Material Available

Comparison of CMAQ predictions and measurements for 12-hour (6 am–6 pm) average  $\text{NH}_3$  concentrations, with a monitoring cycle of 4 days on and 4 days off, at a high emission site

(Kenansville) and a low emission urban site (Raleigh) in North Carolina and comparison of hourly  $\text{NH}_3$  concentrations at a rural SEARCH site (Yorkville) in Georgia (Table S1), Resistance analogue schematic diagrams of dry deposition algorithms: uni-directional flux model; bi-directional flux model where compensation points ( $\chi_s$  and  $\chi_g$ ) replace the infinite sink in the stomata and soil (Figure S1), Interpolated maps of annual average wet deposition of ammonium ( $\text{kg NH}_4 \text{ ha}^{-1}$ ): Interpolated from NADP sites and plotting all CMAQ 12-km cells (Figure S2a), Scatter plot of 2002 annual and summer wet  $\text{NH}_4$  deposition from CMAQ versus NADP. A CMAQ 12-km cell value is paired with the NADP value from the site contained within the CMAQ cell (Figure S2b), Scatter plots of annual average concentrations for 2002 from CMAQ 12-km grids paired with data from the CASTNet and STN networks for  $\text{NH}_4^+$ ,  $\text{SO}_4^{2-}$ ,  $\text{NO}_3^-$  and Total- $\text{NO}_3 = \text{HNO}_3 + \text{NO}_3^-$  (Figure S3), Comparison of CMAQ predictions and measurements for 12-hour (6 am–6 pm) average  $\text{NH}_3$  concentrations, with a monitoring cycle of 4 days on and 4 days off, at a high emission site (Kenansville) and a low emission urban site (Raleigh) in North Carolina compared to CMAQ for July 2004 and August 2004 (Figure S4), Maps of maximum  $V_d$  in each CMAQ 12-km cell for June 25, 2002, unpaired in time, for  $\text{HNO}_3$ ,  $\text{NH}_3$  and  $\text{SO}_2$  (Figure S5), Bar chart of the  $\text{NH}_3$  column budget for the single, isolated Sampson County cell for June 2002:  $\text{SO}_2 = \text{SO}_2 V_d$ ; Bi-Di = Bi-directional; Base = M3dry. Column depth from 0 to 16 km (Figure S6). This information is available free of charge via the internet at <http://www.atmospolres.com>.

## References

- Aneja, V.P., Blunden, J., Roelle, P.A., Schlesinger, W.H., Knighton, R., Niyogi, D., Gilliam, W., Jennings, G., Duke, C.S., 2008. Workshop on agricultural air quality: state of the science. *Atmospheric Environment* 42, 3195-3208.
- Asman, W.A.H., 2001. Modelling the atmospheric transport and deposition of ammonia and ammonium: an overview with special reference to Denmark. *Atmospheric Environment* 35, 1969-1983.
- Asman, W.A.H., 1998. Factors influencing local dry deposition of gases with special reference to ammonia. *Atmospheric Environment* 32, 415-421.
- Byun, D., Schere, K.L., 2006. Review of the governing equations, computational algorithms, and other components of the Models-3 Community Multiscale Air Quality (CMAQ) modeling system. *Applied Mechanics Reviews* 59, 51-77.
- Castro, M.S., Driscoll, C.T., Jordan, T.E., Reay, W.G., Boynton, W.R., Seitzinger, S.P., Styles, R.V., Cable, J.E., 2001. Contribution of atmospheric deposition to the total nitrogen loads to thirty-four estuaries on the Atlantic and Gulf Coasts of the United States. In: Valigura, R.A., Alexander, R.B., Castro, M.S., Myers, T.P., Paerl, H.W., Stacey, P.E., Turner, R.E., (Editors). *Nitrogen Loading in Coastal Water Bodies: An Atmospheric Perspective*. Coastal and Estuarine Studies 57. American Geophysical Union, Washington, DC. pp. 77-106.
- Clarisse, L., Clerbaux, C., Dentener, F., Hurtmans, D., Coheur, P.F., 2009. Global ammonia distribution derived from infrared satellite observations. *Nature Geoscience* 2, 479-483.
- Dennis, R.L., 1997. Using the Regional Acid Deposition Model to Determine the Nitrogen Deposition Airshed of the Chesapeake Bay Watershed, in Baker, J.E. editor, *Atmospheric Deposition to the Great Lakes and Coastal Waters*, Society of Environmental Toxicology and Chemistry, Pensacola, FL, 393-413.
- Dennis, R., Haeuber, R., Blett, T., Cosby, J., Driscoll, C., Sickles, J., Johnston, J., 2007. Sulfur and nitrogen deposition on ecosystems in the United States. *EM: Air and Waste Management Association's Magazine for Environmental Managers*, December 2007, 12-17.
- Driscoll, C.T., Lawrence, G.B., Bulger, A.J., Butler, T.J., Cronan, C.S., Eagar, C., Lambert, K.F., Likens, G.E., Stoddard, J.L., Weathers, K.C., 2001. Acidic deposition in the northeastern United States: sources and inputs, ecosystem effects, and management strategies. *Bioscience* 51, 180-198.
- Dumont, E., Harrison, J.A., Kroeze, C., Bakker, E.J., Seitzinger, S.P., 2005. Global distribution and sources of dissolved inorganic nitrogen export to the coastal zone: results from a spatially explicit, global model. *Global Biogeochemical Cycles* 19, art. no. BG4502.
- Duyzer, J.H., Verhagen, H.L.M., Weststrate, J.H., Bosveld, F.C., 1992. Measurement of the dry deposition flux of  $\text{NH}_3$  on to coniferous forest. *Environmental Pollution* 75, 3-13.
- Flechard, C.R., Fowler, D., Sutton, M.A., Cape, J.N., 1999. A dynamic model of bi-directional ammonia exchange between semi-natural vegetation and the atmosphere. *Quarterly Journal of Royal Meteorological Society* 125, 2611-2641.
- Fowler, D., Pitcairn, C.E.R., Sutton, M.A., Flechard, C., Loubet, B., Munro, R.C., 1998. The mass budget of atmospheric ammonia in woodland within 1 km of livestock buildings. *Environmental Pollution* 102, 343-348.
- Galloway, J.N., Cowling, E.B., 2002. Reactive Nitrogen and the World: 200 years of change. *Ambio* 31, 64-71.
- Gipson, G., 1999. Process Analysis, in Byun, D.W., Ching, J.K.S., editors, Science Algorithms of the EPA Models-3 Community Multiscale Air Quality (CMAQ) Modeling System, EPA Report No. EPA-600/R-99/030, Office of Research and Development, Washington DC, pp 16-1 – 16-38.
- Grell, G.A., Dudhia, J., Stauffer, D.R., 1994. A description of the fifth-generation Penn State/NCAR mesoscale model (MM5). NCAR Tech. Note NCAR/TN-398+STR, p.117 (Available from the National Center for Atmospheric Research, P. O. Box 3000, Boulder, CO 80307.)
- Howarth, R.W., Boyer, E.W., Pabich, W.J., Galloway, J.N., 2002. Nitrogen use in the United States from 1961-2000 and potential future trends, *Ambio* 31, 88-96.
- Loubet, B., Asman, W.A.H., Theobald, M.R., Hertel, O., Tang, Y.S., Robin, P., Hassouna, M., Dammgen, U., Genermont, S., Cellier, P., Sutton, M.A., 2009. Ammonia deposition near hot spots: processes, models and monitoring methods. In: Sutton, M.A., Reis, S., Baker, S.M.H., (editors). *Atmospheric Ammonia: Detecting emission changes and environmental impacts. Results of an Expert Workshop under the Convention on Long-range Transboundary Air Pollution*. Springer, 205-267.
- Lovett, G.M., Tear, T.H., 2008. Threats from Above: Air Pollution Impacts on Ecosystems and Biological Diversity in the Eastern United States. The Nature Conservancy and the Cary Institute of Ecosystem Studies ([www.ecostudies.org/reprints/Threats\\_from\\_Above.pdf](http://www.ecostudies.org/reprints/Threats_from_Above.pdf)).
- Mathur, R., Dennis, R.L., 2003. Seasonal and annual modeling of reduced nitrogen compounds over the eastern United States: emissions, ambient levels, and deposition amounts. *Journal of Geophysical Research D: Atmospheres* 108, ACH 22-1 – ACH 22-19.
- Milford, C., Hargreaves, K.J., Sutton, M.A., Loubet, B., Cellier, P., 2001. Fluxes of  $\text{NH}_3$  and  $\text{CO}_2$  over upland moorland in the vicinity of agricultural land. *Journal of Geophysical Research D: Atmospheres* 106, 24169-24181.
- Nemitz, E., Milford, C., Sutton, M.A., 2001. A two-layer canopy compensation point model for describing bi-directional biosphere-atmospheric exchange of ammonia. *Quarterly Journal of Royal Meteorological Society* 127, 815-833.
- Paerl, H.W., Dennis, R.L., Whittall, D.R., 2002. Atmospheric deposition of nitrogen: implications for nutrient over-enrichment of coastal waters. *Estuaries* 25, 677-693.
- Phillips, S.B., Arya, S.P., Aneja, V.P., 2004. Ammonia flux and dry deposition velocity from near-surface concentration gradient measurements over a grass surface in North Carolina. *Atmospheric Environment* 38, 3469-3480.
- Pinder, R.W., Gilliland, A.B., Dennis, R.L., 2008. Environmental impact of atmospheric  $\text{NH}_3$  emissions under present and future conditions in the Eastern United States. *Geophysical Research Letters* 35, art.no. L12808.
- Pleim, J.E., Xiu, A., 1995. Development and testing of a surface flux and planetary boundary layer model for application in mesoscale models. *Journal of Applied Meteorology* 34, 16-32.

- Pleim, J.E., Xiu, A., Finkelstein, P. L., Otte, T.L., 2001. A coupled land-surface and dry deposition model and comparison to field measurements of surface heat, moisture, and ozone fluxes. *Water, Air, and Soil Pollution: Focus* 1, 243-252.
- Pryor, S.C., Barthelmie, R.J., Sorensen, L.L., Jensen, B., 2001. Ammonia concentrations and fluxes over a forest in the Midwestern USA. *Atmospheric Environment* 35, 5645-5656.
- Ratray, G., Sievering, H., 2001. Dry deposition of ammonia, nitric acid, ammonium, and nitrate to alpine tundra as Niwot Ridge, Colorado. *Atmospheric Environment* 35, 1105-1109.
- Seinfeld, J.H., Pandis, S.N., 1998. *Atmospheric Chemistry and Physics*, John Wiley, Hoboken, NJ, pp. 529-541.
- Sutton, M.A., Fowler, D., Moncrieff, J.B., 1993. The exchange of atmospheric ammonia with vegetated surfaces: I. Unfertilized vegetation. *Quarterly Journal Royal Meteorological Society* 119, 1047-1070.
- Sutton, M.A., Asman, W.A.H., Schjorring, J.K., 1994. Dry deposition of reduced nitrogen. *Tellus* 46B, 255-273.
- Tarrason, L., Nyiri, A., 2008. Transboundary acidification, eutrophication and ground level ozone in Europe in 2006, EMEP Status Report 1/2008, Norwegian Meteorological Institute, electronically available at <http://www.emep.int>.
- van Pul, A., Hertel, O., Geels, C., Dore, A.J., Vieno, M., van Jaarsveld, H.A., Bergstrom, R., Schaap, M., Fagerli, H., 2009. Modelling of the atmospheric transport and deposition of ammonia at a national and regional scale. In: Sutton, M.A., Reis, S., Baker, S.M.H., (editors). *Atmospheric Ammonia: Detecting emission changes and environmental impacts. Results of an Expert Workshop under the Convention on Long-range Transboundary Air Pollution*. Springer, 301-358.
- Vitousek, A.M., Aber, J.D., Howarth, R.W., Likens, G.E., Matson, P.A., Schindler, D.W., Schlesinger, W.H., Tilman, D.G., 1997. Human alteration of the global nitrogen cycle: sources and consequences, *Ecological Applications* 7, 737-750.
- Walker, J.T., Robarge, W.P., Wu, Y., Meyers, T.P., 2006. Measurement of bi-directional ammonia fluxes over soybean using the modified Bowen-ratio technique. *Agricultural and Forest Meteorology* 138, 54-68.
- Walker, J., Spence, P., Kimbrough, S., Robarge, W., 2008. Inferential model estimates of ammonia dry deposition in the vicinity of a swine production facility. *Atmospheric Environment* 42, 3407-3418.
- Wyers, G.P., Erisman, J.W., 1998. Ammonia exchange over coniferous forest. *Atmospheric Environment* 32, 441-451.
- Xiu, A., Pleim, J.E., 2001. Development of a land surface model part I: application in a mesoscale meteorology model. *Journal of Applied Meteorology* 40, 192-209.